Carbon Letters
https://doi.org/10.1007/s42823-023-00616-x

Online ISSN 2233-4998
Print ISSN 1976-4251

ORIGINAL ARTICLE

A vacuum pressure sensor based on graphene/ZnO nanorod Schottky junction

P. Sakthivel[1] · K. Ramachandran[1] · M. Malarvizhi[2] · S. Karuppuchamy[3] · P. Manivel[4]

Received: 28 July 2023 / Revised: 7 September 2023 / Accepted: 14 September 2023

Abstract

We present a practical vacuum pressure sensor based on the Schottky junction using graphene anchored on a vertically aligned zinc oxide nanorod (ZnO-NR). The constructed heterosystem of the Schottky junction showed characteristic rectifying behavior with a Schottky barrier height of 0.64 eV. The current–voltage (*I*–*V*) features of the Schottky junction were measured under various pressures between 1.0×10^{3} and 1.0×10^{-3} mbar. The maximum current of 38.17 mA for the Schottky junction was measured at −4 V under 1.0×10^{-3} mbar. The high current responses are larger than those of the previously reported vacuum pressure sensors based on ZnO nanobelt film, ZnO nanowires, and vertically aligned ZnO nanorod devices. The pressure-sensitive current increases with the vacuum pressure and reaches maximum sensitivity (78.76%) at 1.0×10^{-3} mbar. The sensitivity and repeatability of the Schottky junction were studied by the current–time (*I*–*T*) behavior under variation of vacuum pressure. The sensing mechanism is debated from the surface charge transfer doping effect by oxygen chemisorption. The results suggest that this simple graphene/ZnO-NR Schottky junction device may have potential in the fabrication of vacuum pressure sensor with high sensitivity.

Graphical abstract

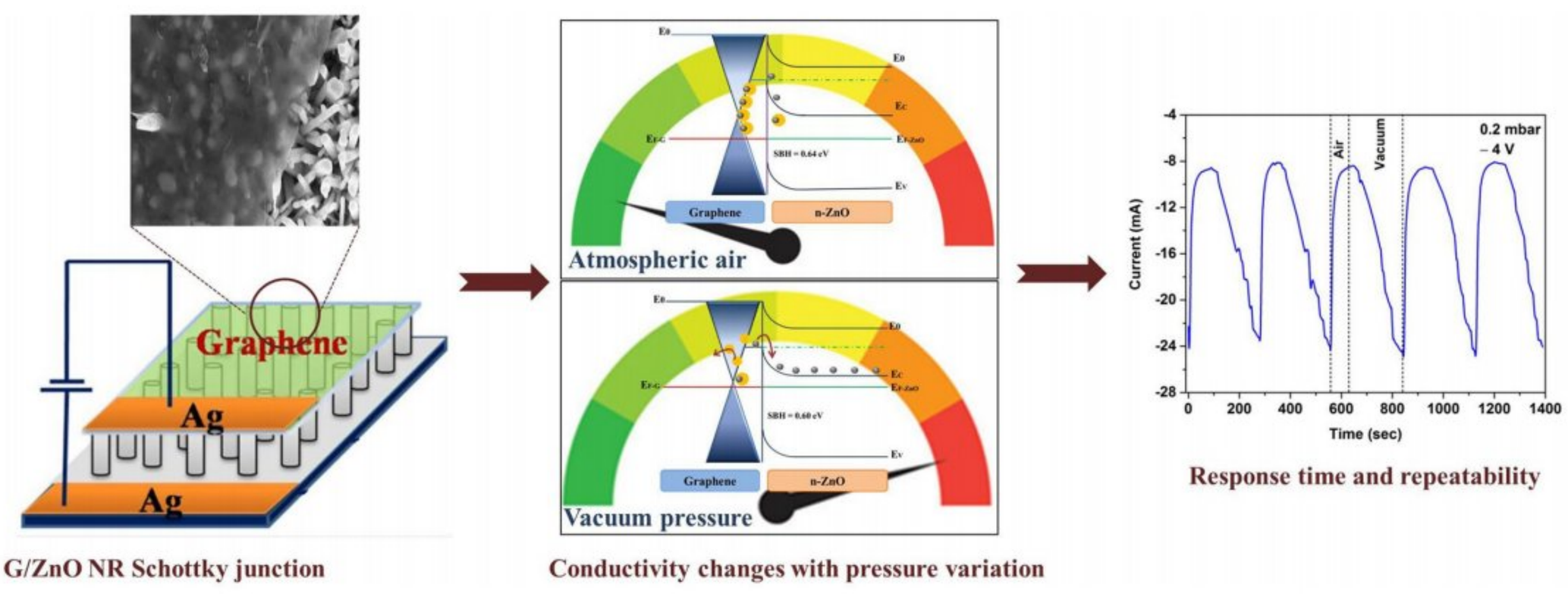

Keywords Graphene · Chemical vapor deposition · ZnO nanorod · Schottky junction · Vacuum pressure sensor

1 Introduction

Recently, there has been a lot of focus on the fabrication of nanostructured electronic devices with well-defined size and shape for sensor applications [1] such as molecular,

Extended author information available on the last page of the article

Published online: 07 October 2023

temperature, various biosensors, and vacuum pressure sensors [2]. Vacuum sensors are important devices and are generally used in thin film deposition, manufacturing control unit, and research. The vacuum pressure sensing process using thermocouples with a hotplate and self-heated Pirani gauge has various effective applications in the industry [3, 4]. Due to the large size, the sensing systems are not suitable for integrated circuit. Interestingly, field-emission (FE), microoptoelectromechanical system (MOEMS), and microelectromechanical system (MEMS) devices [5, 6] were reducing the size of electronic devices. However, the manufacturing complication, operating voltage, and high cost of electronics need to be considered before claims. These problems make it challenging to commercialize FE devices, MOEMS, and MEMS in vacuum sensors [7].

Generally, low-dimensional ZnO nanomaterials are of larger length with a high surface area so that they could provide high current responses in electronic and sensor devices, such as photoconductive switch, oxygen sensors, chemical detector, and self-powered ethanol sensor. There have also been reports of vacuum pressure sensors based on ZnO nanostructured materials such as nanobelt film, nanowires, and vertically aligned nanorods [1, 8, 9]. However, these vacuum pressure sensors are challenging to use in practical applications due to their incredibly weak current response. We naturally explore whether the response current of a vacuum pressure sensor may be improved using a graphene/ZnO-NR Schottky junction, which has more carrier channels in a small region.

Recently, two-dimensional (2D) graphene has been employed in various potential applications due to its extraordinary material properties including remarkably high charge carrier mobility and very high surface area [10]. These properties make widespread interest in their potential applications for gas molecule detection based on conductivity and surface work function. A conventional resistive-type sensor operates based on variation in the electrical resistance of graphene upon gas molecule exposure [11]. However, conventional sensors do not exhibit high sensitivity because the electrical resistance of graphene changes according to the number of transferred charge carriers, which are limited by the density of exchange charge and the characteristics of graphene and gaseous molecules [12].

Heterojunction devices made of graphene and semiconductors have been recently employed in electronic device [13]. Such heterojunctions are not only fundamentally attractive from the perspective of electronic devices but also very promising for sensing applications due to the atomically thin nature of graphene. However, zero-band gap graphene acts as a metal in the heterojunction with semiconductor (e.g., ZnO nanorod) to form the Schottky junction [14]. The sensing signal is magnified by the nonlinear characteristics of the device, which has attracted researchers worldwide to study Schottky junction made of graphene and semiconductors [15]. The earliest studies on metal and semiconductor interfaces were conducted by Schottky and Mott [16, 17]. An energy barrier is created at the interface when a metal and semiconductor come into contact. The Schottky barrier'' height, which also regulates the flow of current over the interface, is determined by the work functions of two different materials. To examine the physical and electrical characteristics of metal/semiconductor materials and their surfaces, Schottky junctions have been employed [18, 19]. However, its presence can enhance or decrease the performance of devices, especially in gas molecule exposure on graphene under atmospheric air and vacuum pressure. Therefore, we consider whether using a high surface area of graphene in contact with ZnO-NR will increase the response of vacuum pressure sensors.

Herein, we fabricated a Schottky junction of graphene/ZnO nanorod (G/ZnO-NR) and investigated its electrical and vacuum pressure sensing characteristics. The resistance–pressure (R–P) and sensitivity–pressure (S–P) curves were established by measuring the current–voltage (I–V) properties at various vacuum pressures. The sensitive mechanism is discussed from the surface charge transfer effect by oxygen chemisorption to understand the large response current of G/ZnO-NR Schottky junction. Also, the stability, repeatability, and reproducibility of G/ZnO-NR Schottky junction sensor were investigated. This research may provide a useful guideline for the potential application of the Schottky junction for designing high-performance vacuum pressure sensors.

2 Experimental methods

2.1 Synthesis of CVD graphene film and ZnO-NR

Graphene films were grown on 25-μm-thick Cu foils (used as the catalytic substrates) using the chemical vapor deposition (CVD) method at 1000 °C with a mixture of C_2H_2 (10 SCCM) and H_2 (200 SCCM) as the reaction source [14]. Following deposition, polymethylmethacrylate (PMMA) solution was spun coated over the graphene films, and the bottom Cu substrate was removed by etching with 0.5 M ammonium persulfate solution. Then, PMMA-supported graphene was applied to the glass substrate and dried at 100 °C for 10 min and the PMMA was removed using acetone. The characteristic structures of the as-synthesized graphene layer were confirmed by Raman spectroscopy with an excitation wavelength of 633 nm.

The ZnO-NR has been formed with 1:1 ratio of amine/Zn by aqueous solution-based growth technique at low temperature [20]. An approximately 100 nm thickness of ZnO seed layer was coated on 1×1 cm^2 selected area of indium

tin oxide (ITO) substrates by RF sputtering. Separately dissolved the hexamine (HMTA) ($C_6H_{12}N_4$) and zinc nitrate hexahydrate Zn $(NO_3)_2 \cdot 6H_2O$ were in double-distilled water and constantly stirred for 15 min. To create a single-phase growth solution, the Zn $(NO_3)_2$ solution and HMTA solution were combined dropwise and continuously stirred for 20 min. The ZnO seed layer-covered ITO substrate was dipped in the growth substance and kept at 95 °C for 5 h. After the growth procedure was complete, the nanorod-deposited substrates were washed with distilled water and ethanol and then they were baked for a further 30 min at 150 °C.

2.2 Characterization

The surface morphologies of the as-synthesized ZnO-NR were characterized by field-emission scanning electron microscopy (FE-SEM, Carl Zeiss Sigma). Phase identification and crystalline orientation were investigated by XRD (Bruker Advanced D8) with Cu-Kα ($\lambda = 0.15406$ nm) radiation in the range of 20–80° at room temperature. Photoluminescence (PL) measurements were obtained using a 32-nm He-Cd laser operating at room temperature.

2.3 Vacuum pressure Sensor fabrication

Graphene/ZnO-NR Schottky junction vacuum pressure sensors were fabricated using as-grown ZnO-NR followed by the transfer of CVD graphene. To make the surfaces of the as-grown ZnO-NR arrays more hydrophilic, they were exposed to oxygen plasma for 30 s at a pressure of 100 torr. The four sides of ZnO-NR were then sealed using sellotape to act as insulation. To mount the 1×1 cm^2 size of PMMA-coated graphene film on top of ZnO-NR arrays, the film was floated in deionized water and progressively elevated. Finally, the contact was developed by silver paste on the graphene sheet after removing PMMA using acetone. The vacuum pressure sensing properties of G/ZnO-NR Schottky junction were analyzed by a simple, home-built vacuum chamber with a rotary pump setup (HINDHIVAC Model: 12 MSPT). The sensor has been placed in a vacuum chamber and coupled to a Keithley 2400 source measurement unit by an ECOPIA Hall probe. The current–voltage features of vacuum sensor were determined under standard atmospheric and various vacuum pressures (1.0×10^3, 5.0×10^{-1}, 2.0×10^{-1}, 1.0×10^{-1}, 5.0×10^{-2}, 1.0×10^{-2}, and 1.0×10^{-3} mbar). To investigate the reproducibility of the vacuum pressure sensor, three separate G/ZnO-NR Schottky junction devices are fabricated with the same conditions and measured current response under different vacuum pressures. The three fabricated G/ZnO-NR Schottky junction devices were named sensor 1, sensor 2, and sensor 3, respectively. The G/ZnO-NR Schottky junction device fabrication process was clearly demonstrated in Scheme 1.

3 Results and discussions

3.1 Structural and morphological studies

The XRD patterns of ZnO-NR made with 1:1 amine/Zn ratios are shown in Fig. 1a. The resulting XRD peaks are in good agreement with the hexagonal wurtzite structure of ZnO identified in JCPDS card 36-1451 [21], and no peaks clearly attributable to contaminants and impurities were found. Compared to other peaks related to the (100) and (004) planes, the (002) plane reflection's strength is rising. This suggests that the *c*-axis perpendicular to the substrate is the preferred direction for one-dimensional nanostructural growth [22].

The quality of the prepared samples has been investigated using micro-Raman measurements. The room temperature Raman spectra of graphene and graphene atop ZnO-NRs are shown in Fig. 1b. The Raman spectra of graphene clearly show that it has three distinctive bands that are located at 1363 cm^{-1} (D), 1578 cm^{-1} (G), and 2722 cm^{-1} (2D), respectively. Typically, defects are attributed to the D band, and disorders in the sp^2 carbon rings emerge. The dispersion of first-order phonons (E2g), often known as G-bands, results in the other G-bands. The other band results from the dispersion of first-order phonons (E2g), often known as G-bands [23, 24]. The two phonon double resonant scatter processes are accountable for the 2D band, which indicates the stacked layer of graphene. However, because of graphene's inherent flaws, the double resonant scatter with elastic and inelastic components that occurs in the D band is possible. As a result, a D band's wave number position is about half of a 2D band and is dependent on the excitation wavelength [25, 26]. Along with the D, G, and 2D bands of graphene, the ZnO mode's characteristics may be seen after the assembly of graphene on ZnO-NRs. The optical phonon E2 (high) mode of the ZnO-NR wurtzite hexagonal phase is clearly seen in the band at 437 cm^{-1}, as illustrated in Fig. 1b [27]. In reality, the presence of defects in layered graphene is almost unavoidable during the CVD growth process. This defective graphene strongly interacts with gas molecules and thus enhances the sensitivity of the Schottky junction device for monitoring vacuum pressure.

The FE-SEM image of the ZnO-NR, CVD graphene, and G/ZnO-NR is shown in Fig. 2. The FE-SEM image of well-defined hexagonal-shaped ZnO-NR with diameters of ~ 100 to 200 nm is shown in Fig. 2a. The excellent quality of the ZnO-NRs is illustrated by great density and homogeneity. Figure 2b displays a FE-SEM image of large-scale graphene that has been transferred to glass. The graphene appears to

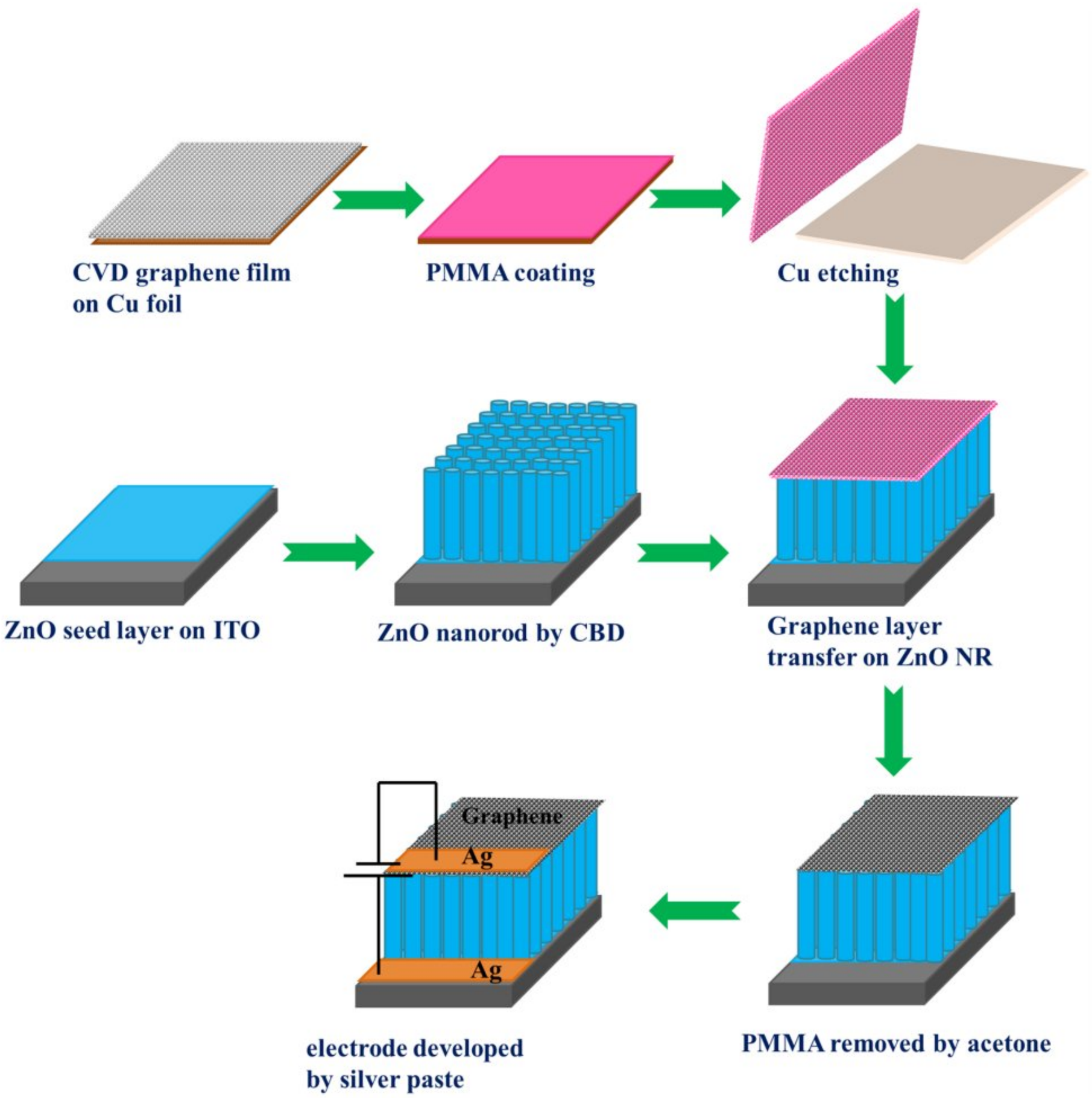

Scheme 1 Fabrication process of G/ZnO-NR Schottky junction device

be continuous in scale, and there are no color contrasts visible using an optical microscope, indicating uniform growth across the sample. However, a few wrinkles in graphene are ascribed to the process of wet chemical transferring the graphene layer. Also, we examined the hybrid G/ZnO-NR using FE-SEM. The resultant features, as depicted in Fig. 2c, d, demonstrate the greater homogeneity of graphene over the transferred region without any fractures or openings. However, the random wrinkle features that have been noticed are unavoidably created during the process of transfer and do not appear to have any effect on the sensor device.

The effectiveness of charge carrier entrapment and the lifetime of photogenerated electron–hole pairs from semiconductors under light irradiation are commonly investigated using the PL emission spectrum [28]. Figure 3 shows the PL spectra of G/ZnO-NR and bare ZnO-NR, which were both obtained at room temperature using a He-Cd laser at an excitation wavelength of 325 nm. The UV emission peak in the PL spectra of G/ZnO-NR is identical to those of bare ZnO-NR. The broad and intense emission peak was observed at 383 nm, and it was caused by the direct recombination process of electron and hole pairs. After anchoring the graphene on ZnO-NR, the emission intensity of the G/ZnO-NR was dramatically reduced. It is evident from the outstanding interaction between graphene and ZnO-NR [29, 30].

3.2 Vacuum pressure sensor studies

Figure 4 shows the *I*–*V* plots of the vacuum sensor at normal atmospheric pressure and different low pressures.

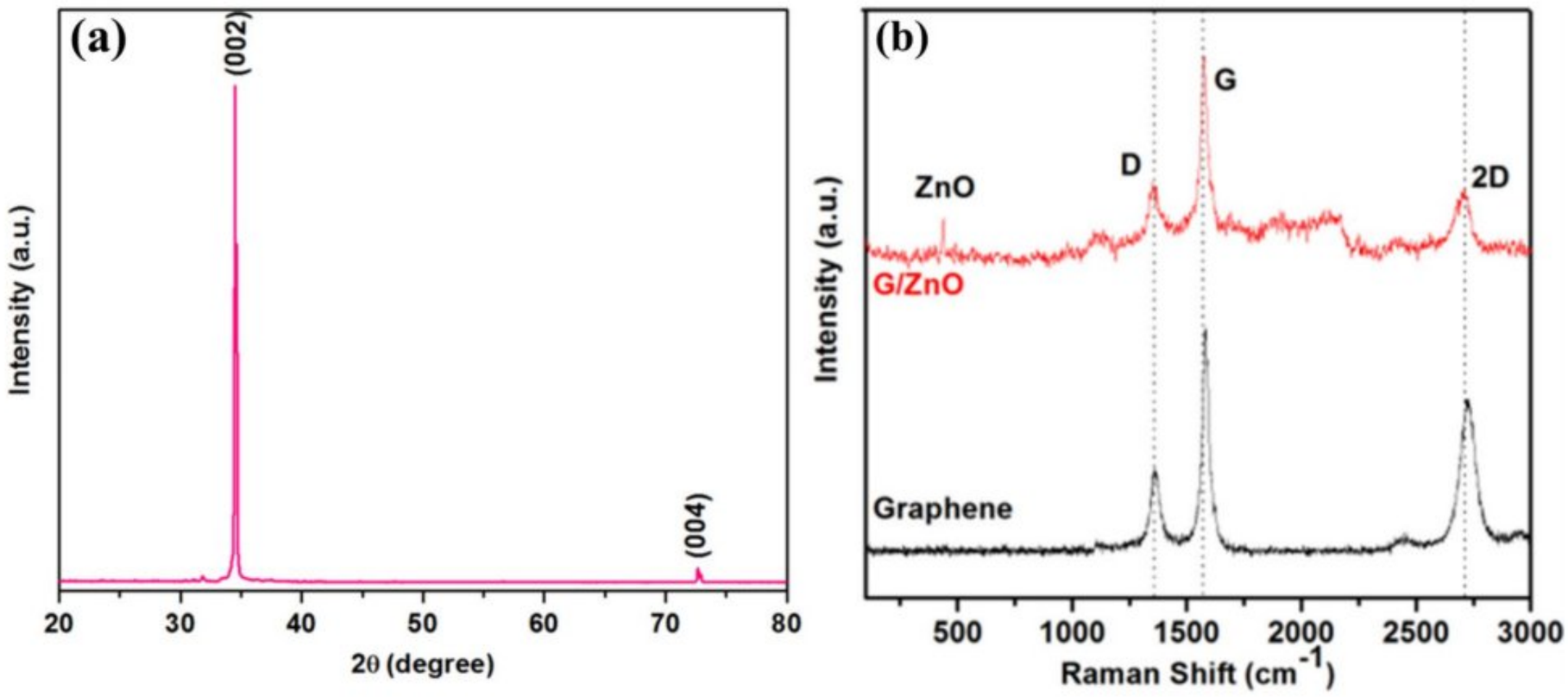

Fig. 1 **a** X-ray diffraction pattern of ZnO-NR and **b** Raman spectra of CVD graphene and G/ZnO-NR

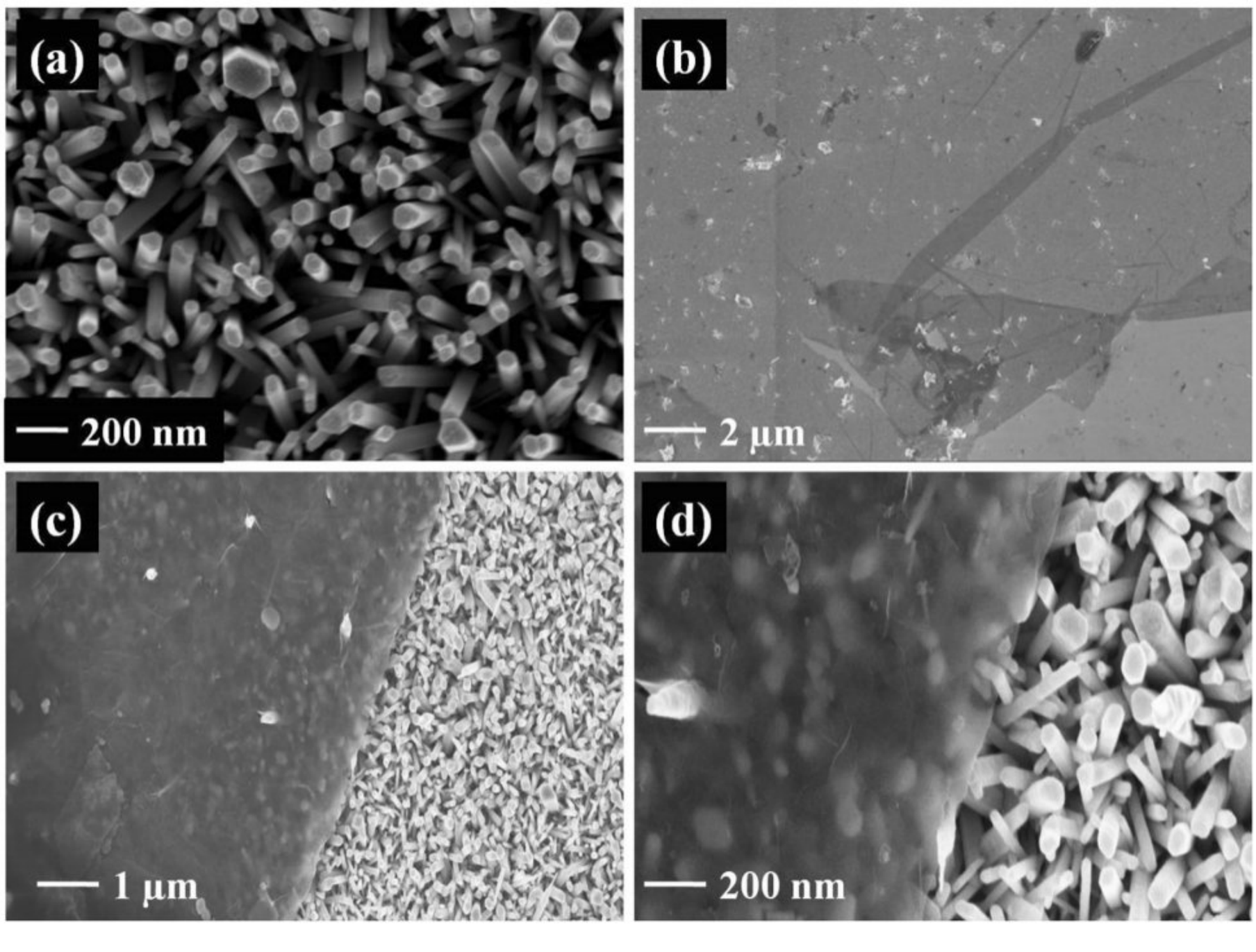

Fig. 2 FE-SEM image of **a** ZnO-NR, **b** CVD graphene, and **c**, **d** low and high magnification of G/ZnO-NR

The inset of Fig. 4a shows the G/ZnO-NR Schottky junction structure. A typical rectifying contact between graphene and ZnO-NR is depicted in Fig. 4a, with a Schottky barrier height (SBH) of 0.64 eV. The thermionic emission model can be used to explain the rectifying behavior of the G/ZnO-NR contact [31], which is expressed as follows:

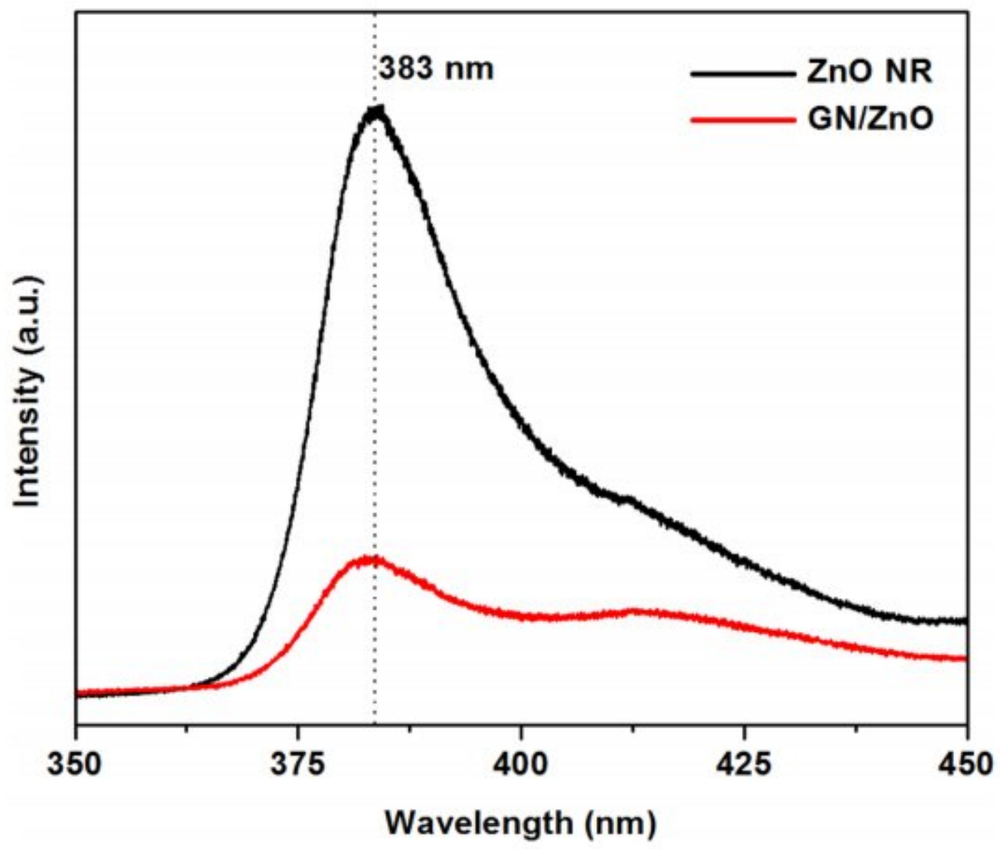

Fig. 3 Photoluminescence spectra of ZnO-NR and G/ZnO-NR

$$I = I_S\left[\exp\left(\frac{qV}{\eta K_B T}\right) - 1\right] \quad (1)$$

where I_S is the saturation current, q is the electron charge, η is the ideality factor, k is the Boltzmann constant, and T is the absolute temperature. As shown in Fig. 4b, the current response drastically increases with the increase in chamber vacuum pressure at −4 V. The current value is significantly high (38.17 mA) under vacuum pressures of 1×10^{-3} mbar. The current response of the G/ZnO-NR Schottky junction sensor at 1×10^{-3} mbar is about four orders higher than that of 1×10^{3} mbar. A new kind of stable and sensitive vacuum pressure sensor based on G/ZnO-NR Schottky junction can be developed as a result of the high sensitivity, which shows that the current changes dramatically with the pressure.

The Schottky barrier has to be highly sensitive to oxygen. Consequently, the G/ZnO-NR Schottky device's *I–V* curves were measured at atmospheric air and vacuum pressure to further confirm the presence of the Schottky barrier in our

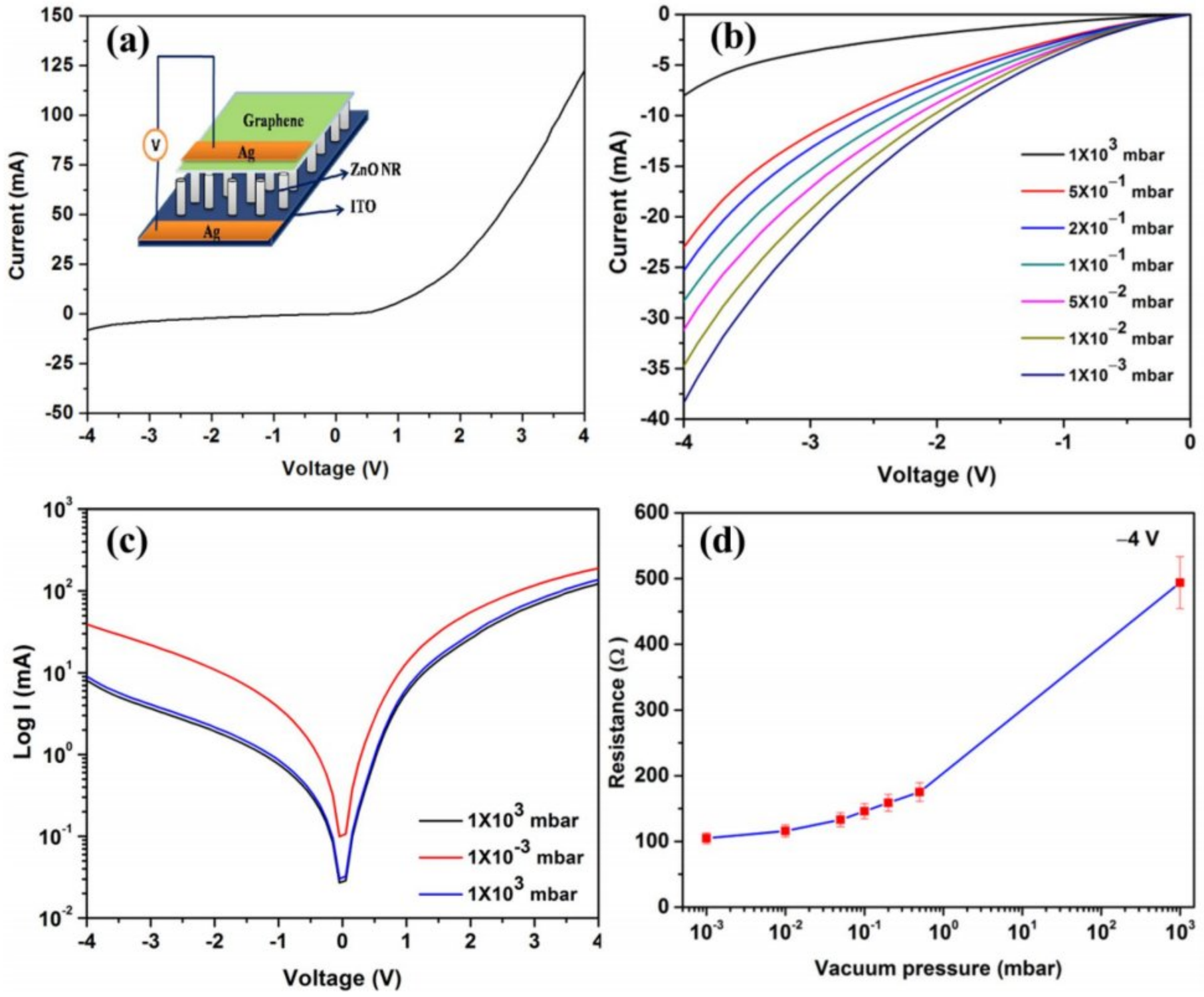

Fig. 4 **a** *I–V* characteristic of G/ZnO-NR junction at atmospheric air (inset: G/ZnO-NR Schottky junction); **b** *I–V* curves of G/ZnO-NR Schottky junction at different pressures of 1.0×10^{3}, 5.0×10^{-1}, 2.0×10^{-1}, 1.0×10^{-1}, 5.0×10^{-2}, 1.0×10^{-2}, and 1.0×10^{-3} mbar; **c** log *I–V* curve of G/ZnO-NR junction under atmospheric air and vacuum pressure; and **d** *R–P* relationship of G/ZnO-NR Schottky junction

devices as shown in Fig. 4c. The G/ZnO-NR Schottky junction showed significantly improved conductivity in vacuum, which is due to the Schottky barriers' extreme sensitivity to O_2 gas [32]. Once the device was back in contact with air, the conductivity totally comes back to its original level due to the Schottky barrier's quick recovery. However, both the ZnO-NR resistance and the Schottky barrier have an influence on the conductivity. Additionally, the noticed little conductivity is due to the ZnO-NR sluggish recovery. Furthermore, the resistance R can be obtained by Ohmic law from Fig. 4b, and the logarithmical relationship between the resistance and pressure (*R*–*P* curve) is summarized as shown in Fig. 4d. The curve shows that the electrical resistance of the G/ZnO-NR Schottky device decreased monotonically with pressure. This observation shows that the sensor is sensitive from atmospheric pressure to vacuum.

In general, the chemisorption mechanism plays an important role in regulating the conductance of sensitive nanoscale devices. The adsorption and desorption of gas molecules such as NH_3, CO_2, H_2O, and O_2 can change the transport characteristics of graphene [33]. The oxygen molecule is a well-known accepting electron to induce doping effects, which could influence the Fermi level (E_F) of graphene [34, 35]. However, the position of the Fermi level varied by the density of electron in the current transport of graphene [24]. As a result, oxygen chemisorption and desorption control the charge transfer effect in the G/ZnO-NR Schottky device sensor, which may be utilized to interpret changes in the E_F of graphene under vacuum pressure. The sensitive mechanism of G/ZnO-NR Schottky junction can be explained with the help of schematic energy band diagram as shown in Fig. 5. In atmospheric air, a lot of oxygen molecules are adsorbed on the exposed surface of the graphene layer, and they capture free electrons to become negatively charged oxygen ions. The negatively charged oxygen ions will reduce the number of free electrons that cross interface, which leads to a decrease in the conductivity because the E_F is shifted toward the valence band of ZnO-NR. In a vacuum, the air is extracted by a rotary pump to lower the amount of oxygen molecules in the chamber and the oxygen molecules at the graphene surface will be desorbed or diffused into the air. In this process, the captured electrons are released from the negatively charged oxygen ions to enhance the conducting carrier's density. It may lead to a shift in the E_F toward the conduction band of ZnO-NR, which would increase conductivity [18]. With the increase in the vacuum pressure in the chamber, more and more oxygen molecules are desorbed from the surface of graphene to reduce the barrier height of the Schottky junction; therefore, the enhanced conductivity will increase the current as in Fig. 4b and decrease the resistance as in Fig. 4d.

The sensitivity $S = \left(R_a - R_V\right)/R_a \times 100$ can be used to calculate the sensor's sensitivity, where R_a and R_V represent the resistance of the constructed Schottky device under a standard atmosphere and vacuum pressure, respectively. From Fig. 4b, the sensitivities S are correspondingly calculated as 64.5, 67.8, 70.4, 73.0, 76.5, and 78.7% under 5.0×10^{-1}, 2.0×10^{-1}, 1.0×10^{-1}, 5.0×10^{-2}, 1.0×10^{-2}, and 1.0×10^{-3} mbar, and then, the *S*–*P* relationship of vacuum pressure sensor based on G/ZnO-NR Schottky junction can be given in Fig. 6a. This new kind of vacuum pressure sensor could be developed with improved high sensitivity (78.76%) at 1.0×10^{-3} mbar, which indicates that the current response changes dramatically from atmospheric pressure to vacuum pressure.

To explore the repeatability and response time of G/ZnO-NR Schottky junction sensor the *I*–*T* was measured for five cycles at −4 V under vacuum pressure variation

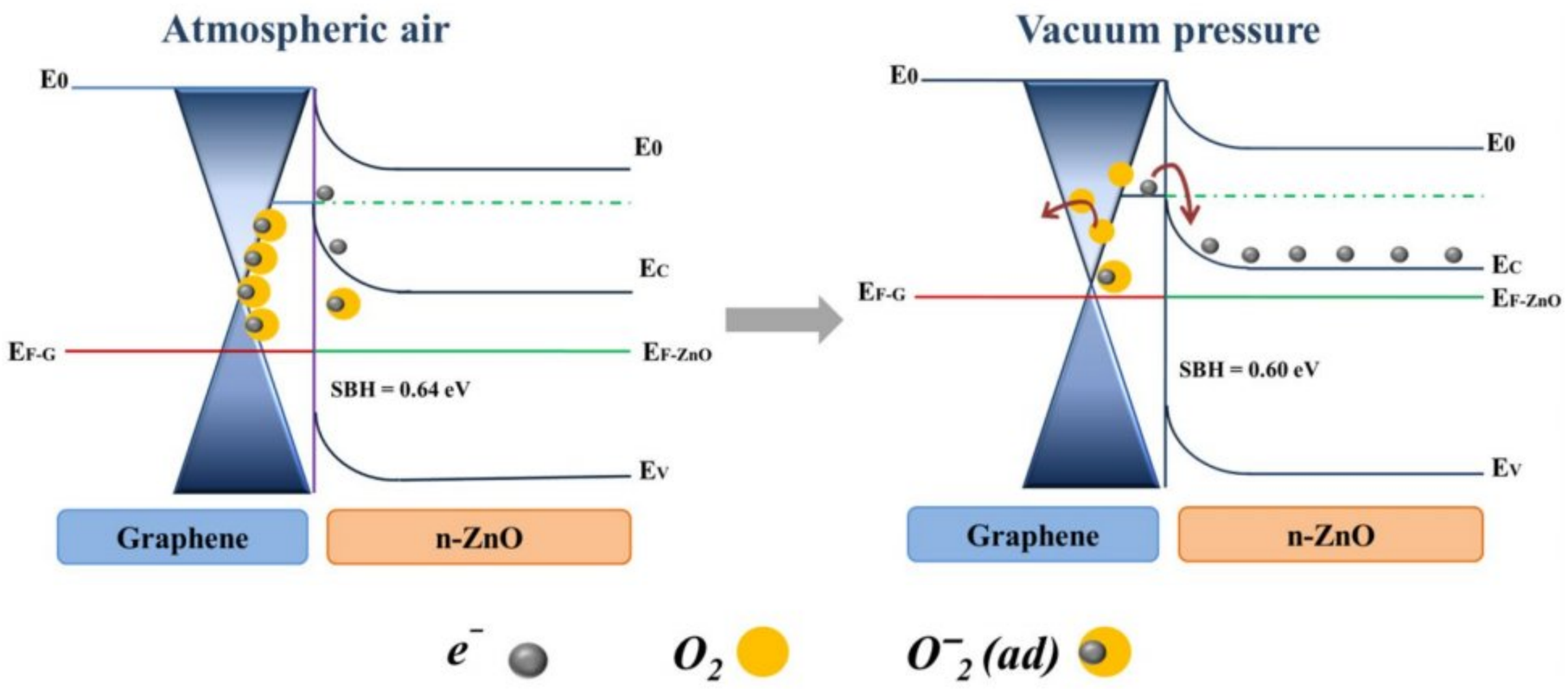

Fig. 5 A Schematic diagram of the vacuum pressure-sensitive mechanism of G/ZnO-NR Schottky junction under atmospheric air and vacuum pressure

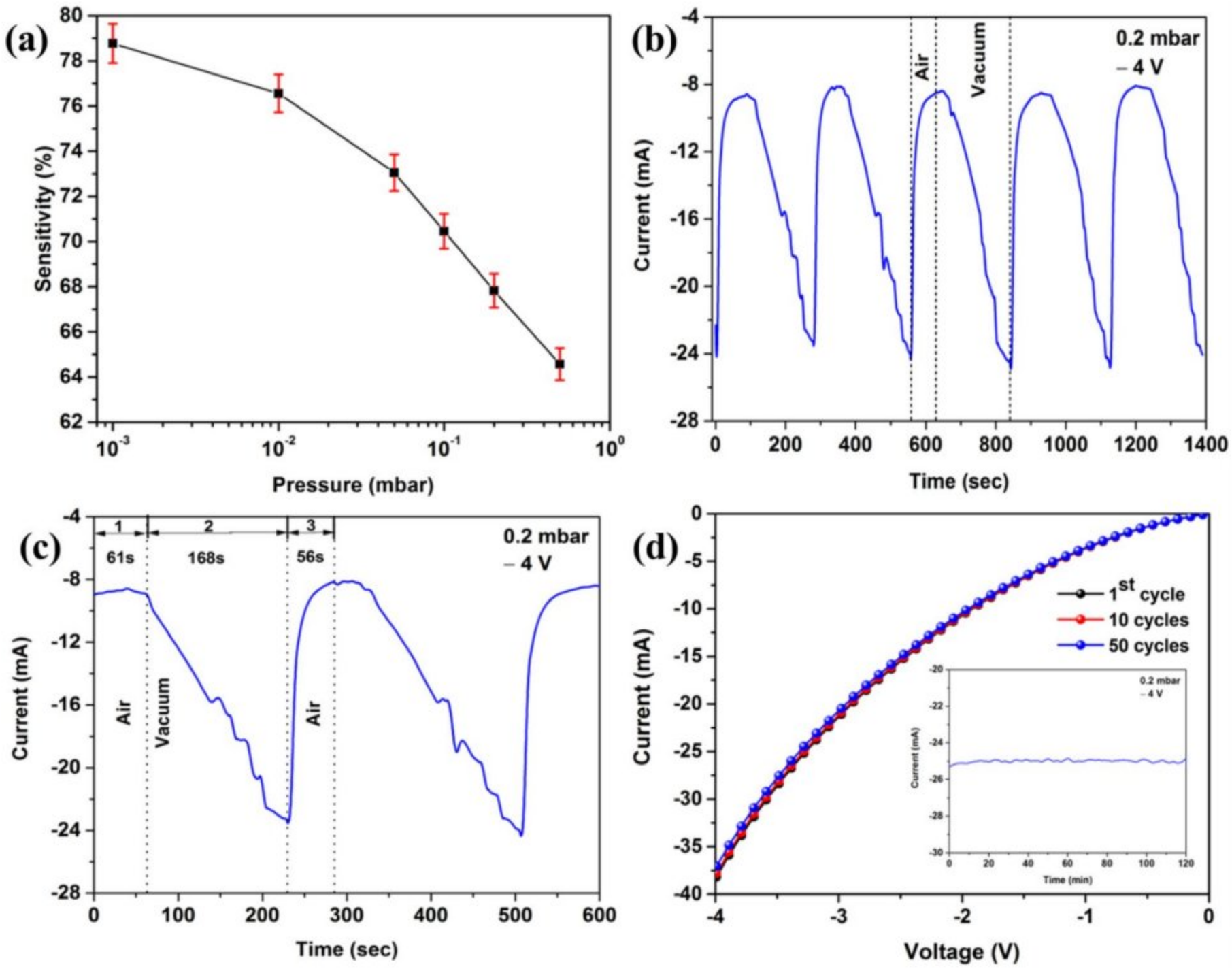

Fig. 6 **a** *S–P* relationship, **b**, **c** *I–T* curves of G/ZnO-NR Schottky junction with pressure variation, and **d** *I–V* curve of G/ZnO-NR Schottky junction before and after 50 cycles, and (insert) the *I–T* responses of G/ZnO-NR Schottky junction at the applied bias of − 4 V under 2.0×10^{-1} mbar

as shown in Fig. 6b, c. There are approximately the same current fluctuations, which indicate that the signal is repeatable. The response currents are steady at 8.89 mA under atmospheric pressure for the sensors based on G/ZnO-NR Schottky junction after turning off the rotary pump within the range of 0–61 s for step 1. The response currents significantly increase (24.5 mA) with increasing vacuum pressure from the atmospheric pressure to 2.0×10^{-1} mbar within the range of 61–229 s for step 2 after opening the valve and turning on the rotary pump. Therefore, the response time of the G/ZnO-NR Schottky junction sensors is ~ 0.14 mA/s. After turning off the rotary pump and allowing atmospheric air to chamber, the response currents recover to the steady value of 8.87 mA with a small fluctuation through 56 s for Step 3. The sensor currents change continuously with pressure variation, which indicates a good response and recovery time with good repeatability.

Apart from sensing performance, stability is also an important parameter to evaluate the performance of electrocatalysts. As shown in Fig. 6d, the current density (*I–V*) maintains almost identical to its initial curve after 50 cycles, demonstrating the superior stability of G/ZnO-NR Schottky junction sensor and possibilities for practical applications. Furthermore, the long-term stability was observed by *I–T* measurement at − 0.2 V for the period of 120 min (inset Fig. 6d). The *I–T* curve of G/ZnO-NR Schottky junction shows good stability, and there was no significant drop in the overall current trend. The slight fluctuation of curve may be due to the variation in the maintained pressure level.

To prove the reproducibility of vacuum pressure sensor, three separate G/ZnO-NR Schottky junction devices are fabricated and their current responses were measured in *I–V* characteristics under various vacuum pressures. The current response drastically increases with the increase in vacuum pressure as shown in Fig. 7. The current value is found similarly for all three sensors without significant changes. The obtained maximum current values of three sensors under 1.0×10^{-3} mbar are about 38.17, 36.70, and 39.71 mA for sensor 1, sensor 2, and sensor 3, respectively. Figure 7d demonstrates the histogram plot for comparison of three sensors'

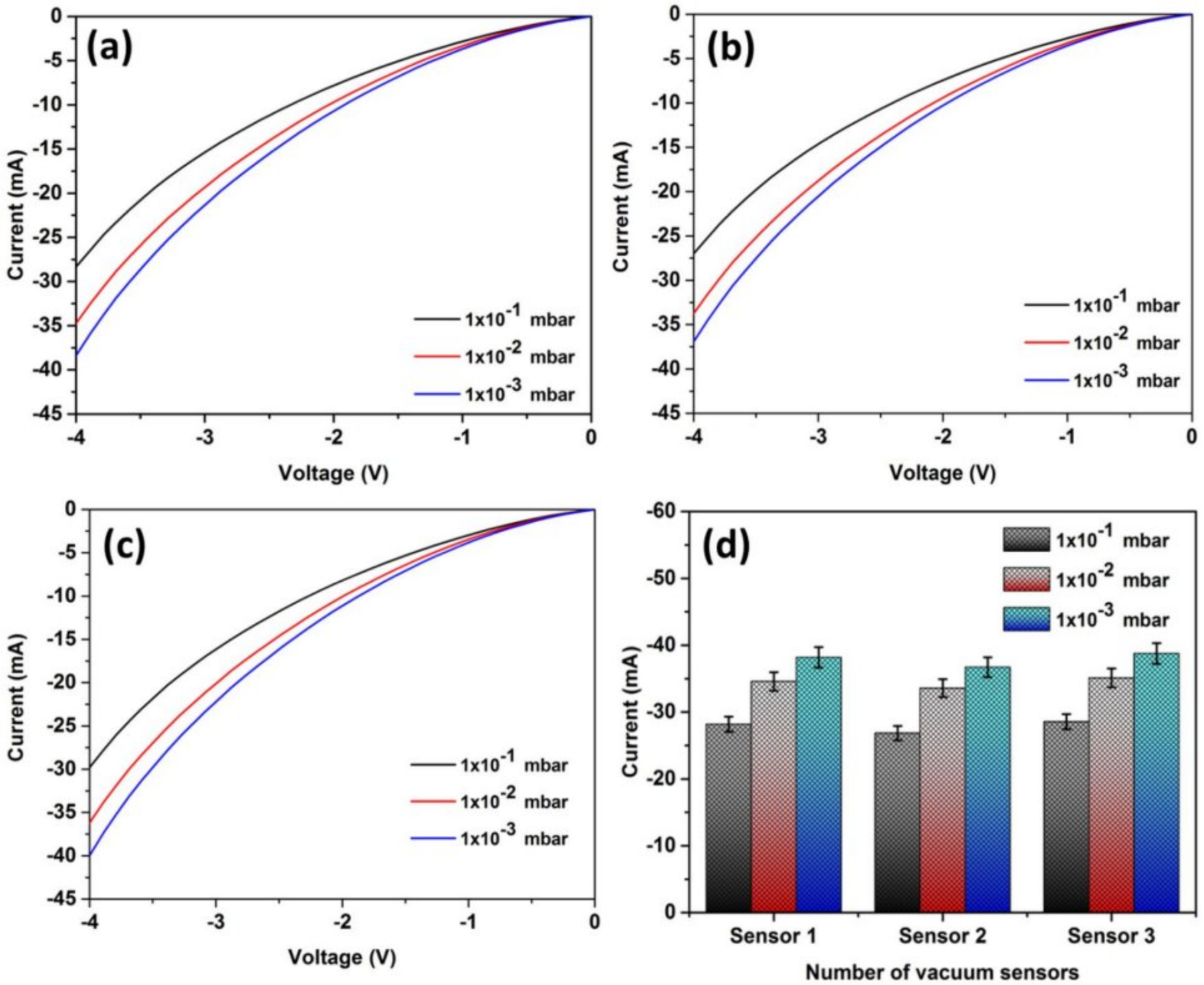

Fig. 7 *I–V* curve of G/ZnO-NR Schottky junction sensor at different pressures of 1.0×10^{-1}, 1.0×10^{-2}, and 1.0×10^{-3} mbar. **a** Sensor 1, **b** sensor 2, and **c** sensor 3. **d** Histogram graph of three G/ZnO-NR Schottky junction for reproducibility

current response at − 4 V under different vacuum pressures. There is a small current variation between three sensors about 1–2.5 mA due to the Schottky barrier height and E_F level, defects, and layer properties of CVD-grown graphene.

Vacuum pressure sensors play a significant role in modern industrial development. However, there are still many challenges to the applicability of vacuum pressure sensors due to their integration techniques, complex fabrication, mass production, and high cost. In recent years, ZnO and graphene-based vacuum pressure sensors have been interested, which proposed a good sensing response. For instance, ZnO nanostructured-based vacuum pressure sensor fabricated through the lithographic process has evidence of a significant current response [7, 36]. However, fabrication costs and device integrity greatly hinder vacuum pressure sensors' commercial and practical applications. The low-temperature solution-grown ZnO-NR has excellent potential for fabricating devices because of its scalability and shortened fabrication time. In addition, easy fabrication of the Schottky junction on ZnO-NR through transferring CVD graphene film promoted the device integrity with a simple strategy and low-cost fabrication technique. Also, this simple fabrication process makes mass production and scalability of G/ZnO-NR Schottky junction-based device assembly. The integrated G/ZnO-NR Schottky junction-based vacuum pressure sensor with distinguished features such as high sensitivity, nanoscale feature, low cost, and simple fabrication shows great feasibility, and it may be a tremendous potential candidate for vacuum technology in modern industries such as switches, pneumatic conveying, packaging, and degassing.

4 Conclusion

We present a simple G/ZnO-NR Schottky junction vacuum pressure sensor. The as-fabricated device demonstrated a characteristic rectifying performance, with a SBH of 0.64 eV. The sensor response significantly increases with the increase in chamber vacuum pressure at − 4 V. The Schottky junction sensor sensitivity increased to 78.76% with good response and recovery as the chamber vacuum pressure was varied. The oxygen chemisorption on the surface of the

graphene with the charge transfer doping effect was used to explain the mechanism of pressure sensitivity. The G/ZnO-NR-based Schottky junction suggested in this paper shows promise for a novel class of vacuum pressure sensor.

Data availability The datasets used and/or analyzed during the current study are available from the corresponding author on reasonable request.

Declarations

Conflict of interest The authors declare that they have no conflict of interest.

References

1. Wang D, Zheng X, Cao X, Wang X, Zhang T (2016) The large response current of a vacuum pressure sensor based on a vertically-aligned ZnO nanowires array. RSC Adv 6:114566–114571. https://doi.org/10.1039/C6RA18433B
2. Ahn SI, Jung J, Kim Y, Lee Y, Kim K, Lee SE, Kim S, Choi KK (2016) Self-assembled and intercalated film of reduced graphene oxide for a novel vacuum pressure sensor. Sci Rep 6:38830–38836. https://doi.org/10.1038/srep38830
3. Xu S, Na Z, Shi M, Zhang C, Chen D, Mao H (2022) Overview of the MEMS Pirani sensors. Micromachines 13:945. https://doi.org/10.3390/mi13060945
4. Sun X, Xu D, Xiong B, Wu G, Wang Y (2013) A wide measurement pressure range CMOS-MEMS based integrated thermopile vacuum gauge with an XeF_2 dry-etching process. Sens Actuator A Phys 201:428–433. https://doi.org/10.1016/j.sna.2013.07.020
5. Chircov C, Grumezescu AM (2022) Microelectromechanical systems (MEMS) for biomedical applications. Micromachines 13:164. https://doi.org/10.3390/mi13020164
6. Xu M, Feng Y, Han X, Ke X, Li G, Zeng Y, Yan H, Li D (2021) Design and fabrication of an absolute pressure MEMS capacitance vacuum sensor based on silicon bonding technology. Vacuum 186:110065. https://doi.org/10.1016/j.vacuum.2021.110065
7. Chang SJ, Hsueh TJ, Hsu CL, Lin YR, Chen IC, Huang BR (2008) A ZnO nanowire vacuum pressure sensor. Nanotechnology 19:095505. https://doi.org/10.1088/0957-4484/19/9/095505
8. Zheng XJ, Cao XC, Sun J, Yuan B, Li QH, Zhu Z, Zhang Y (2011) A vacuum pressure sensor based on ZnO nanobelt film. Nanotechnology 22:435501. https://doi.org/10.1088/0957-4484/22/43/435501
9. Wu L, Song FF, Fang X, Guo ZX, Liang S (2010) A practical vacuum sensor based on a ZnO nanowire array. Nanotechnology 21:475502. https://doi.org/10.1088/0957-4484/21/47/475502
10. Tiwari SK, Sahoo S, Wang N, Huczko A (2020) Graphene research and their outputs: status and prospect. J SCI-ADV Mater Dev 5:10–29. https://doi.org/10.1016/j.jsamd.2020.01.006
11. Ghosh R, Aslam M, Kalita H (2022) Graphene derivatives for chemiresistive gas sensors: a review. Mater Today Commun 30:103182. https://doi.org/10.1016/j.mtcomm.2022.103182
12. Quang VV, Trong NS, Trung NN, Hoa ND, Duy NV, Hieu NV (2014) Full-layer controlled synthesis and transfer of large-scale monolayer graphene for nitrogen dioxide and ammonia sensing. Anal Lett 47:280–294. https://doi.org/10.1080/00032719.2013.832270
13. Jahangir I, Uddin MA, Franken A, Singh AK, Koley G (2023) Investigation of graphene/InN nanowire based mixed dimensional barristors with widely tunable Schottky barrier for highly sensitive multimodal gas sensing applications. Sens Actuators B Chem 379:133238. https://doi.org/10.1016/j.snb.2022.133238
14. Li L, Wang J, Yang P (2023) Graphene/Janus ZnO heterostructure to build highly efficient photovoltaic properties. Diam Relat Mater 136:110037. https://doi.org/10.1016/j.diamond.2023.110037
15. Kang SB, Sanger A, Jeong MH, Baik JM, Choi KJ (2023) Heterogeneous stacking of reduced graphene oxide on ZnO nanowires for NO_2 gas sensors with dramatically improved response and high sensitivity. Sens Actuators B Chem 379:133196. https://doi.org/10.1016/j.snb.2022.133196
16. Schottky W (1938) Halbleitertheorie der Sperrschicht. Naturwissenschaften 26:843. https://doi.org/10.1007/BF01774216
17. Mott NF (1938) Note on the contact between a metal and an insulator or semi-conductor. Math Proc Camb Philos Soc 34:568–572. https://doi.org/10.1017/S0305004100020570
18. Kim HY, Lee K, McEvoy N, Yim C, Duesberg GS (2013) Chemically modulated graphene diodes. Nano Lett 13:2182–2188. https://doi.org/10.1021/nl400674k
19. Gupta S, Knoepfel A, Zou H, Ding Y (2023) Investigations of methane gas sensor based on biasing operation of n-ZnO nanorods/p-Si assembled diode and Pd functionalized Schottky junctions. Sens Actuators B Chem 392:134030. https://doi.org/10.1016/j.snb.2023.134030
20. Ranjith KS, Pandian R, McGlynn E, Rajendra Kumar RT (2014) Alignment, morphology and defect control of vertically aligned ZnO nanorod array: competition between "surfactant" and "stabilizer" roles of the amine species and its photocatalytic properties. Cryst Growth Des 14:2873–2879. https://doi.org/10.1021/cg5001792
21. Yan D, Xu PC, Xiang Q, Mou HM, Xu JQ, Wen WJ, Li XX, Zhang Y (2016) Polydopamine nanotubes: bio-inspired synthesis, formaldehyde sensing properties and thermodynamic investigation. J Mater Chem A 4:3487–3493. https://doi.org/10.1039/C6TA00396F
22. Gill R, Ghosh S, Sharma A, Kumar D, Nguyen VH, Vo DVN, Pham TD, Kumar P (2020) Vertically aligned ZnO nanorods for photoelectrochemical water splitting application. Mater Lett 277:128295. https://doi.org/10.1016/j.matlet.2020.128295
23. Fouda AN, El Basaty AB, Eid EA (2016) Photo-response of functionalized self-assembled graphene oxide on zinc oxide heterostructure to UV illumination. Nanoscale Res Lett 11:13. https://doi.org/10.1186/s11671-015-1221-8
24. Duraia E-SM, Beall GW (2015) Humidity sensing properties of reduced humic acid. Sens Actuators B Chem 220:22–26. https://doi.org/10.1016/j.snb.2015.05.028
25. Ramírez C, Shamshirgar AS, Pérez-Coll D, Osendi MI, Miranzo P, Tewari GC, Karppinen M, Hussainova I, Belmonte M (2023) CVD nanocrystalline multilayer graphene coated 3D-printed alumina lattices. Carbon 202:36–46. https://doi.org/10.1016/j.carbon.2022.10.085
26. Thy LTM, Giang NT, Hang N, Nhiem LT (2023) Defect engineering of CVD graphene and real-time Raman study of NO_2 adsorption toward enhanced sensing sensitivity. FlatChem 39:100505. https://doi.org/10.1016/j.flatc.2023.100505
27. Ramadoss A, Kim SJ (2013) Facile preparation and electrochemical characterization of graphene/ZnO nanocomposite for supercapacitor applications. Mater Chem Phys 140:405–411
28. Abd-Elrahim AG, Chun DM (2021) Facile one-step deposition of ZnO-graphene nanosheets hybrid photoanodes for enhanced photoelectrochemical water splitting. J Alloys Compd 870:159430. https://doi.org/10.1016/j.jallcom.2021.159430
29. Gao C, Zhong K, Fang X, Fang D, Zhao H, Wang D, Li B, Zhai Y, Chu X, Li J, Wang X (2021) Brief review of photocatalysis and photoresponse properties of ZnO–graphene nanocomposites. Energies 14:6403. https://doi.org/10.3390/en14196403

30. Busarello P, Quadros S, Zimmermann LM, Neiva EGC (2023) Graphene oxide/ZnO nanocomposites applied in photocatalysis of dyes: tailoring aqueous stability of quantum dots. Colloids Surf A Physicochem Eng 675:132026. https://doi.org/10.1016/j.colsurfa.2023.132026
31. Dharmaraj P, Jesuraj PJ, Jeganathan K (2016) Tuning a Schottky barrier of epitaxial graphene/4H-SiC (0001) by hydrogen intercalation. Appl Phys Lett 108:051605. https://doi.org/10.1063/1.4941229
32. Fu XW, Liao ZM, Zhou YB, Wu HC, Bie YQ, Xu J, Yu DP (2012) Graphene/ZnO nanowire/graphene vertical structure based fast-response ultraviolet photodetector. Appl Phys Lett 100:223114. https://doi.org/10.1063/1.4724208
33. Zitoune H, Adessi C, Benchallal L, Samah M (2021) Quantum transport properties of gas molecules adsorbed on Fe doped arm-chair graphene nanoribbons: a first principle study. J Phys Chem Solids 153:109996. https://doi.org/10.1016/j.jpcs.2021.109996
34. Hua Ni Z, Wang HM, Luo ZQ, Wang YY, Yu T, Wu YH, Shena ZX (2010) The effect of vacuum annealing on graphene. J Raman Spectrosc 41:479–483. https://doi.org/10.1002/jrs.2485
35. Shin DW, Lee HM, Yu SM, Lim KS, Jung JH, Kim MK, Kim SW, Han JH, Ruoff RS, Yoo JB (2012) A facile route to recover intrinsic graphene over large scale. ACS Nano 6:7781–7788. https://doi.org/10.1021/nn3017603
36. Sarcan F (2020) ZnO nanoparticles-based vacuum pressure sensor. Nanotechnology 31:435502. https://doi.org/10.1088/1361-6528/aba39d

Authors and Affiliations

P. Sakthivel[1] · K. Ramachandran[1] · M. Malarvizhi[2] · S. Karuppuchamy[3] · P. Manivel[4]

✉ P. Manivel
maninano@gmail.com

[1] Department of Chemistry, Builders Engineering College, Tirupur, Tamil Nadu 638 108, India

[2] Department of Chemistry, Sri GVG Visalakshi College for Women, Udumalpet, Tamil Nadu 642 128, India

[3] Department of Energy Science, Alagappa University, Karaikudi, Tamil Nadu 630 003, India

[4] Centre for Nanotechnology, Erode Sengunthar Engineering College, Erode, Tamil Nadu 638 057, India